



Precision electrochemical machining of tungsten micro-rods using wire electrochemical turning method

Wei Han¹ · Masanori Kunieda¹

Received: 18 April 2020 / Accepted: 20 September 2020 / Published online: 26 September 2020
© Springer-Verlag London Ltd., part of Springer Nature 2020

Abstract

The novel wire electrochemical turning (WECT) method has been proposed to machine tungsten with neutral electrolyte and bipolar pulse current in the authors' previous research. The influence of tool wear caused by the bipolar pulse current, which is needed to remove the oxide layer generated on tungsten surface when using a neutral electrolyte, was eliminated by the WECT method because the wire tool electrode was kept being wound during the machining process. In this paper, the influences of the most important process parameters, such as the kind of electrolyte, wire material, wire diameter, rotation speed of the workpiece rod, and frequency of the pulse voltage, were studied to understand the fundamental aspects of the WECT method and improve the machining efficiency of tungsten micro-rods. The experimental results showed that the NaCl electrolyte and the NaNO₃ electrolyte had higher machining efficiency and better machining accuracy, respectively. The machining accuracy was improved with the SUS304 stainless steel wire used as tool electrode than the brass wire tool electrode. It was also found that the machining efficiency and accuracy were improved with decreasing the wire diameter and increasing the rotation speed of workpiece because the influence of stray current flowing through the side and end surface of machined micro-rod was reduced. The machinable length of micro-rod peaked at an optimum feed speed of the workpiece, and the optimum speed increased with increasing the frequency of pulse voltage. As a result, a minimum rod diameter of 11 μm was fabricated with a high aspect ratio of 36. Compared with the previous method using a platinum film as tool electrode, the aspect ratio was increased significantly because the influence of tool wear was eliminated.

Keywords Wire electrochemical turning · Electrochemical machining · Tungsten · Micromachining · Electrostatic induction feeding method

1 Introduction

Tungsten has a unique set of properties like the second highest melting point next to carbon among all elements, high elastic modulus, high density, high thermal conductivity, and excellent mechanical properties at elevated temperatures [1]. These exceptional properties make tungsten to be widely used in the fields of optics, micro-electronics, mechanical manufacturing,

and aerospace [2]. In recent years, tungsten has also been used as promising alternative materials for plasma facing components in fusion reactors, owing to its high melting point and low sputtering yield [3]. However, tungsten has a major drawback of significantly low ductility at room temperature and high ductile-to-brittle transition temperature. In addition, tungsten has a high Vickers hardness of 310. Therefore, the poor ductility and high hardness result in poor machinability of tungsten. With the traditional mechanical machining methods, such as cutting, grinding, and milling, the issue of tool wear limits the industrial application and deteriorates the machining accuracy. Zhong et al. [4] reported that the two of the prime challenges in cutting of pure tungsten are high tool wear associated with the reactivity between tungsten and tool materials and its high hardness.

Wire electrical discharge machining (WEDM) as an important non-traditional machining method has provided an effective solution for machining hard materials, e.g., tungsten,

✉ Wei Han
hanwei_wh@edm.t.u-tokyo.ac.jp

Masanori Kunieda
kunieda@edm.t.u-tokyo.ac.jp

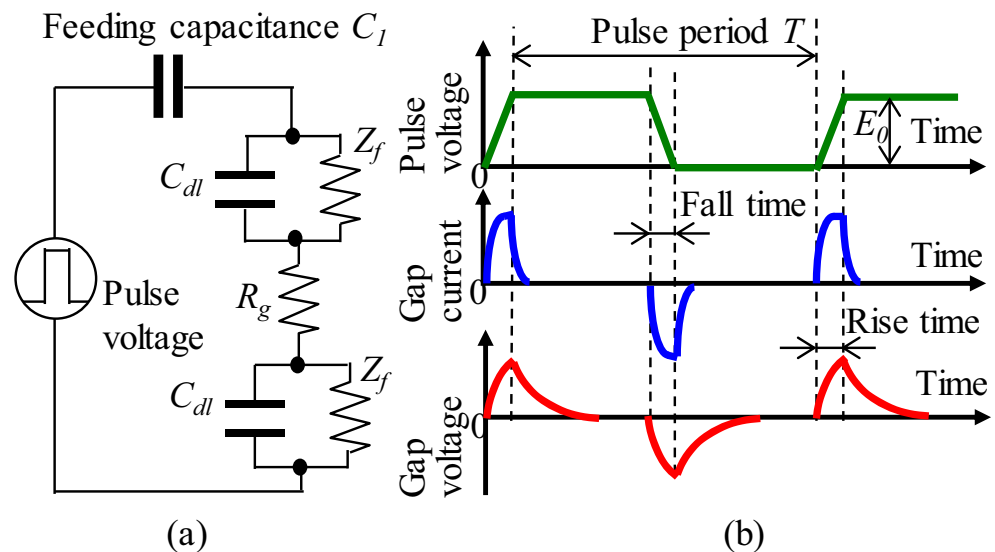
¹ Department of Precision Engineering, The University of Tokyo, Room 833, Engineering Building 14#, 7-3-1, Hongo, Bunkyo-ku, Tokyo 113-8656, Japan

titanium, and molybdenum, with intricate shapes and profiles that are difficult to machine using traditional methods [5, 6]. However, WEDM is a thermal process which results in the poor surface quality such as residual stresses, micro-cracks, and heat-affected zone, and the tool wear problem [7]. Electrochemical machining (ECM) is an alternative method to machine tungsten without the influences of residual stresses, tool wear, and heat-affected zone compared with EDM method because ECM is an anodic dissolution process. Furthermore, ECM has many advantages over other traditional machining methods such as its applicability regardless of material hardness, no tool wear, high material removal rate, smooth and bright surface, and production of components of complex geometry [8]. For the ECM of tungsten, alkaline aqueous solutions such as KOH and NaOH were often used as electrolyte [9, 10] because the tungsten oxide layer generated on the workpiece surface, which interrupts the electrochemical dissolution process, should be removed. However, the use of these alkaline electrolytes is not environmentally acceptable. Hence, Maeda et al. [11] reported that cemented tungsten carbide can be machined with a neutral electrolyte using a bipolar current, because NaOH is generated over the cathode surface when the tungsten carbide electrode is in negative polarity, thereby removing the oxide layer from the surface of tungsten carbide. Based on the principle proposed by Maeda et al., Han and Kunieda [12] machined tungsten successfully using a neutral electrolyte sodium nitrate (NaNO_3) aqueous solution with the help of a bipolar current supplied by the electrostatic induction feeding method. Kunieda et al. [13] developed the electrostatic induction feeding method used for micro-EDM to decrease the diameters of discharge craters by eliminating the influence of stray capacitance in electric feeders. It is known that ultra-short pulse current can improve the machining accuracy in micro-ECM process through

localizing the electrochemical dissolution in a narrower working gap due to the electrical double layer formed on the surfaces of electrodes [14]. Thus, Koyano and Kunieda [15] applied the electrostatic induction feeding method to generate the ultra-short pulse current in micro-ECM, as shown in Fig. 1. The working gap is modelled using the capacitance of electric double-layer C_{dl} , Faraday impedance Z_f , and electrolyte resistance R_g . Current flows through the working gap only at the instance when the pulse voltage changes to high or low because the pulse power supply is coupled to the tool electrode by a feeding capacitance C_f , as shown in Fig. 1(a). Hence, the current pulse duration is nearly equal to the rise and fall time regardless of the pulse on-time of the pulse voltage, as shown in Fig. 1(b). With this method, short current pulses of several tens of nanoseconds can easily be obtained, without the use of an expensive ultra-short pulse generator. Furthermore, this method has the advantage that the generated ultra-short pulse current is bipolar, which is useful for the ECM of tungsten with a neutral electrolyte. However, the used bipolar current caused tool wear when the tool electrode was in a positive polarity. Hence, Han and Kunieda [16] proposed a novel wire electrochemical grinding (WECG) method to eliminate the influence of tool wear by using a winding wire as tool electrode, which was based on the wire electro-discharge grinding (WEDG) method [17]. The experimental results showed that the wire tool electrode was slightly worn with the applied bipolar pulse current, but the worn area could be reduced significantly with increasing the winding speed of the wire tool electrode. Hence, the influence of the tool wear on the machining accuracy was eliminated with the proposed WECG method.

However, the published paper [16] has not studied the machining characteristics of the WECG method in details. Hence, the achievable limits of miniaturization and aspect

Fig. 1 Principle of electrostatic induction feeding ECM. (a) Equivalent circuit. (b) Gap current and voltage waveforms



ratio of micro-rods machined by the proposed method have not been investigated yet. Those limits are important for the applications of producing micro-rods, such as the probes for scanning probe microscopes (SPM) and tools used for micro-milling, blanking, and EDM. Thus, this paper focuses on the investigation of the fundamental machining characteristics and the limits of minimum rod diameter and aspect ratio obtained using this method. The influences of different electrolyte types, tool electrode material, diameter of wire tool electrode, rotation speed of workpiece rod, and the frequency of pulse voltage on the machining efficiency and accuracy are investigated. Thereby, the present research aims to fabricate the minimum rod diameter with high aspect ratio based on the above results.

2 Wire electrochemical turning method

Figure 2 shows the idea of the present method which was proposed in the previous paper [16] and originally named as wire electrochemical grinding (WECG) after the well-established wire electro-discharge grinding (WEDG) method [17]. However, the naming is changed to wire electrochemical turning (WECT) in this paper because turning is more appropriate to express its principle. The micro-EDM machine (Panasonic, MG-ED72W) with a positioning resolution of $0.1\ \mu\text{m}$ for x , y , and z axis was retrofitted to the micro-ECM machine by replacing the EDM pulse generator with the electrostatic induction feeding method in Fig. 1(a). A wire winding system which was developed by Masuzawa et al. [17] for the WEDG method was installed under the help of Takeshi Technology Institution, Japan. The workpiece rod was fixed in a mandrel supported by V-shape ceramic guides and rotated

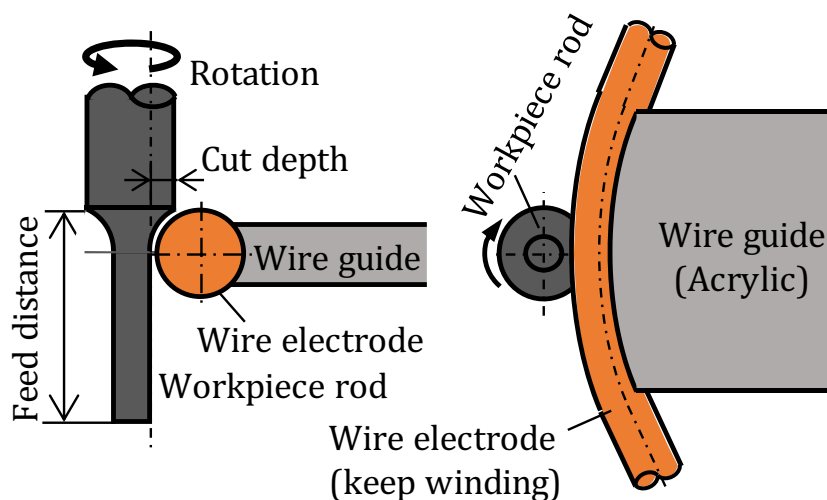
up to 3000 rpm with sufficiently small run-out under $0.5\ \mu\text{m}$, and the wire tool electrode was held by a wire guide made of acrylic. The electrolyte was jetted into the working gap from a nozzle placed near to the working area with an inner diameter of $210\ \mu\text{m}$. A rectangular pulse generated by a function generator (Agilent, 33250A) was amplified by a bipolar amplifier (NF Corporation, HSA4101) used as the pulse voltage supply. A silver mica capacitor was used for the feeding capacitance C_f . A commercial SUS304 stainless steel or brass wire with a diameter of 50 or $100\ \mu\text{m}$ was used as tool electrode and it was kept being wound during the machining process with a winding speed of $11.3\ \text{mm/min}$. Since the wire tool electrode was kept being wound, the influence of tool wear caused by the bipolar pulse current on the machining process could be eliminated. The workpiece rod was positioned over the top surface of the wire tool electrode with an initial gap width of $5\ \mu\text{m}$ before machining and fed toward the wire tool electrode during machining. The cut depth in the radial direction determines the machined rod diameter and the feed distance in the axial direction determines the rod length. The ultra-short pulse bipolar current in the working gap was supplied using the electrostatic induction feeding method, as shown in Fig. 1(b).

3 Influence of different kinds of neutral electrolyte

3.1 Experimental method

The influences of different kinds of neutral electrolytes, sodium nitrate (NaNO_3) and sodium chloride (NaCl) aqueous solutions, on the machining characteristics were investigated. The workpiece was commercial pure tungsten rod with an

Fig. 2 Wire electrochemical turning (WECT) method



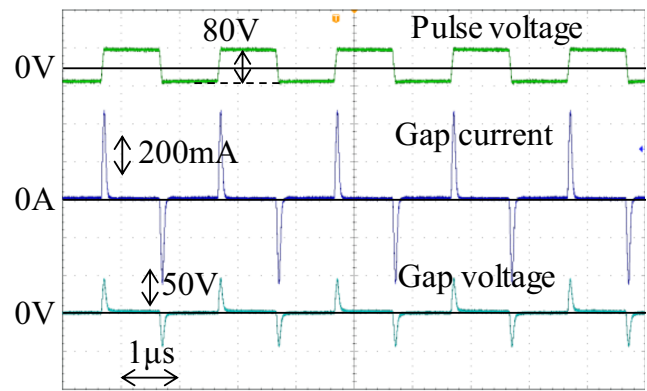
original diameter of 300 μm and length of 50 mm. It was reshaped using the WEDG method [17] to make it sufficiently straight, resulting in a reshaped size of 200 μm in diameter and 400 μm in length. Table 1 shows the experimental conditions used for WECT. The total amplitude of the pulse voltage was 80 V with the frequency of 500 kHz. The duty factor, which was defined as the percentage of the positive pulse time in a pulse period, was 50%. The rise/fall time of the pulse voltage was 40 ns, which would determine the width of the ultra-short pulse current flowing through the working gap. The feeding capacitance C_f used for the electrostatic induction feeding method, as shown in Fig. 1(a), was 350 pF. A commercial SUS304 stainless steel wire of 100 μm in diameter was used as the tool electrode. The NaNO_3 and NaCl aqueous solutions of 6 wt% in concentration were used as electrolytes. The cut depth in the radial direction was 60 μm and the feed distance in the axial direction was 300 μm . The feed speed of the workpiece in the axial direction was increased from 0.1 to 0.5 $\mu\text{m/s}$.

3.2 Experimental results

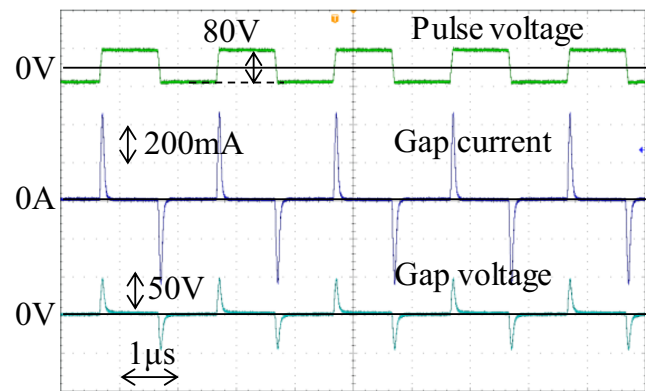
Figure 3 shows the waveforms of gap current and voltage with different kinds of electrolyte at the feed speed of 0.2 $\mu\text{m/s}$. It is found that the difference in the gap currents was slight with different kinds of electrolyte. Figure 4 shows the machinable lengths of micro-rods with different kinds of electrolyte. The machinable length is defined as the finally fabricated length of micro-rod with the given voltage and feed speed. The machinable length is the sum of the feeding distance of workpiece and the axial gap width at the end of machining when the machining completes without collision between electrodes. When the machining is interrupted by collision, the feed distance until collision was considered to be equal to the machinable length. When NaNO_3 aqueous solution was used, the preset feed distance of 300 μm was reached only with the low feed speeds of 0.1 $\mu\text{m/s}$ and 0.2 $\mu\text{m/s}$. With the feed speed higher than 0.2 $\mu\text{m/s}$, the collision occurred between the electrodes before the feed distance reached 300 μm . It is found that the machinable length of micro-rod was longer with the electrolyte of NaCl aqueous solution than that with the electrolyte of NaNO_3 aqueous solution with the feed speed higher than 0.2 $\mu\text{m/s}$. This is because the current efficiency of NaCl

Table 1 Experimental conditions used for studying different kinds of neutral electrolytes

Pulse voltage	Amplitude (V)	80
	Frequency (kHz)	500
	Duty factor (%)	50
	Rise/fall time (ns)	40
Feeding capacitance C_f (pF)		350
Workpiece electrode rotation (rpm)		3000



(a)



(b)

Fig. 3 Waveforms of gap current and voltage with different kinds of electrolyte. (a) NaNO_3 electrolyte. (b) NaCl electrolyte

aqueous solution was higher than the NaNO_3 aqueous solution, especially with a low current density [18, 19]. Han and Kunieda [20] also found that the material removal rate of NaCl electrolyte was higher than the NaNO_3 aqueous solution when machining the SUS304 stainless steel rod using the ECM method which used a thin film as the tool electrode due to the higher current efficiency of NaCl aqueous solution. Figure 5 shows the micro-rods machined with different kinds of electrolyte at the feed speed of 0.2 $\mu\text{m/s}$. It is noted that the end edge of the micro-rod machined with the NaCl electrolyte was rounded, as shown in Fig. 5(b), while Fig. 5(a) shows a

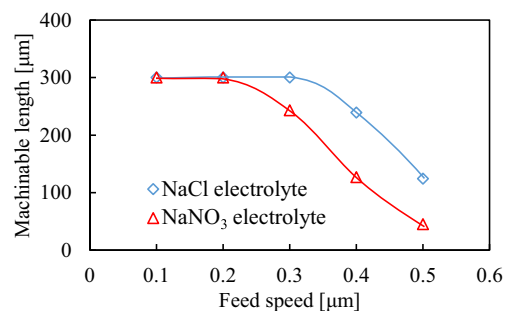
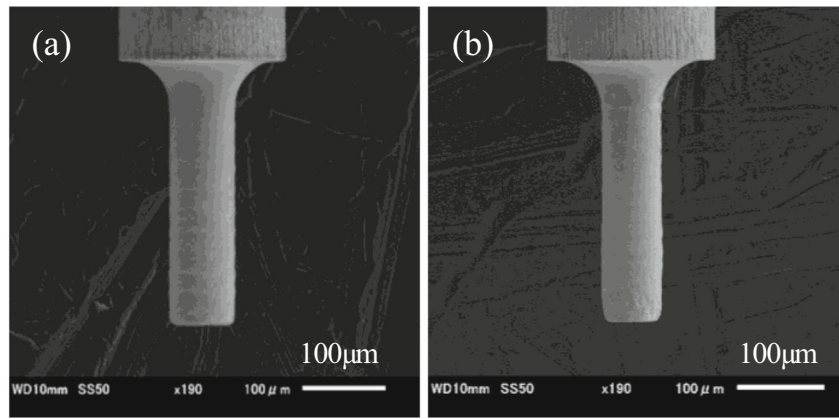


Fig. 4 Machinable lengths of micro-rods with different kinds of electrolyte

Fig. 5 Micro-rod machined with different kinds of electrolyte of (a) NaNO₃ and (b) NaCl aqueous solutions



higher shape accuracy at the end edge with the electrolyte of NaNO₃ aqueous solution. Because of the higher current efficiency of NaCl aqueous solution independent of the current density, the electrochemical dissolution occurred even in a larger working gap width, thereby more workpiece material was dissolved than the NaNO₃ aqueous solution due to the stray current. In addition, the higher current efficiency resulted in wider axial and radial gap widths, which would deteriorate the machining accuracy. Figure 6 shows the axial and radial gap widths with different kinds of electrolyte. The gap widths were larger with the NaCl electrolyte. With both the electrolytes, the radial gap widths were larger than the axial gap widths because the workpiece electrode was fed in the axial direction. The radial gap width G_r and axial gap width G_a were calculated by the following equations.

$$G_r = \frac{D-d}{2} - C_r \tag{1}$$

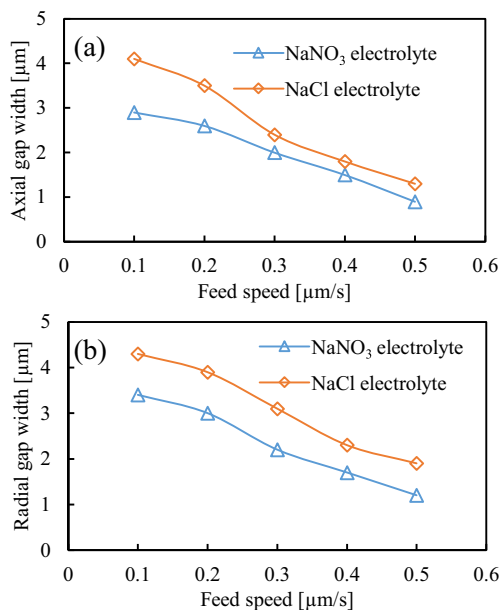


Fig. 6 a Axial and b radial gap widths with different kinds of electrolyte

$$G_a = L - F_a + G_i \tag{2}$$

where D is the diameter of reshaped workpiece rod by the WEDG method, d is the diameter of micro-rod machined by the WECT method, C_r is the preset cut depth in the radial direction before machining, L is the machined length of micro-rod, F_a is the feed distance in the axial direction after machining, and G_i is the initial gap width before machining.

4 Influence of material of wire tool electrode

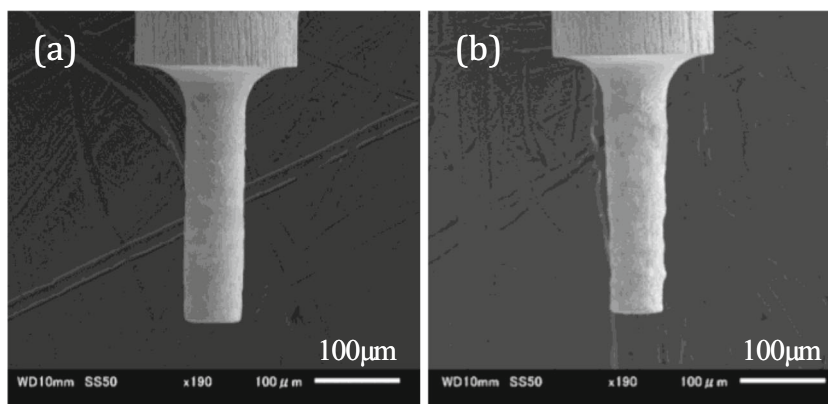
4.1 Experimental method

The same experimental conditions in Table 1 were used in this section. Moreover, SUS304 stainless steel and brass wires with the diameter of 50 μm were used as the wire tool electrode. The NaNO₃ aqueous solution 6 wt% in concentration was used as electrolyte due to the machining accuracy higher than NaCl electrolyte as shown in Section 3. The feed speed of workpiece in the axial direction was 0.1 μm/s. The cut depth in the radial direction and feed distance in the axial direction were 30 μm and 300 μm, respectively.

4.2 Experimental results

Figure 7 shows the micro-rods machined with different wire materials at the feed speed of 0.1 μm/s. The side surface of the micro-rod obtained with the brass wire tool electrode was not sufficiently straight compared with that with the SUS304 stainless steel wire electrode. It is speculated that this was partly related to the tool material dissolution when the polarity of the wire electrode was positive by the use of the bipolar pulse current. Figure 8 shows the brass and SUS304 stainless steel wire tool electrodes before and after machining. It is found that the wire material is dissolved more significantly with the brass

Fig. 7 Micro-rods machined with (a) SUS304 stainless steel and (b) brass wire tool electrode



wire tool electrode. Therefore, the SUS304 stainless steel wire was used as the tool electrode in all the following experiments due to the better machining accuracy.

5 Influence of diameter of wire tool electrode

5.1 Experimental method

To study the influence of the diameter of wire tool electrode on the machining accuracy, the diameter was changed at 50 μm and 100 μm . The wire material was SUS304 stainless steel due to the better performance in

machining accuracy, as discussed in Section 4. The feed speed of workpiece in the axial direction was increased from 0.1 to 0.6 $\mu\text{m}/\text{s}$ with an increment of 0.1 $\mu\text{m}/\text{s}$, while the other machining conditions were the same to Table 2, such as the pulse voltage and electrolyte.

5.2 Experimental results

Figure 9 shows the waveforms of the gap current and voltage with different diameters of wire tool electrode. The gap current increased with increasing the wire diameter. This is because the axial gap area increased with increasing the wire diameter. The decrease in the gap

Fig. 8 Brass and SUS304 stainless steel wire tool electrodes before and after machining. (a) Brass wire tool electrode. (b) SUS304 wire tool electrode

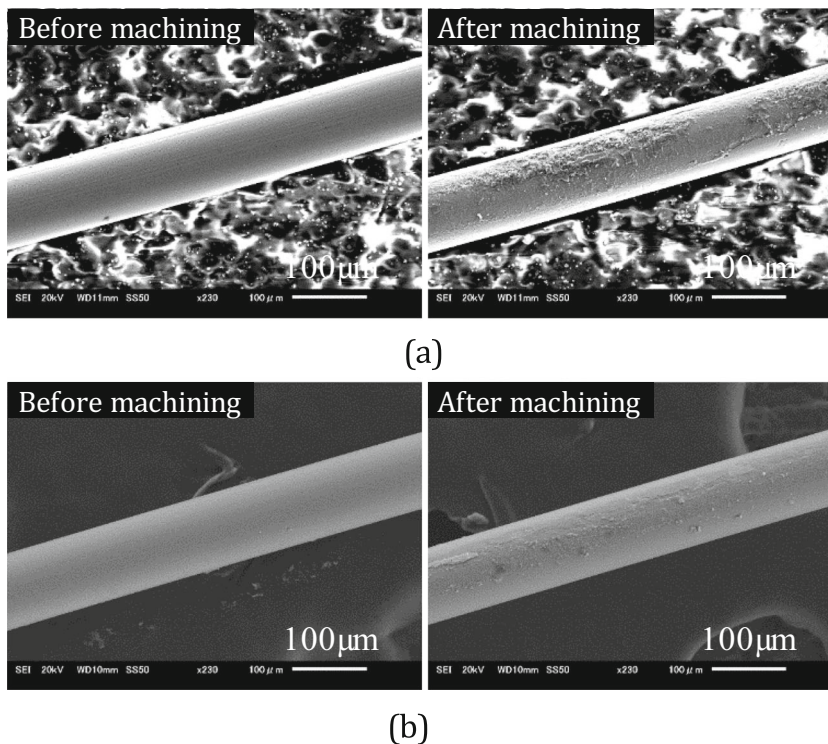


Table 2 Experimental conditions used to investigate the influence of rotation speed of workpiece

Pulse voltage	Amplitude (V)	70
	Frequency (kHz)	500
	Duty factor (%)	50
	Rise/fall time (ns)	20
Feeding capacitance C_f (pF)	350	
Electrolyte	NaNO ₃ aq. 3 wt%	
Wire tool electrode	SUS304 stainless steel wire ϕ 50 μ m	

resistance due to the larger axial gap area resulted in the higher gap current as shown in Fig. 10. It is noted that the stray current, which flows through the radial gap, also increased with increasing the wire diameter due to the larger radial gap area. It is also found that the pulse duration with the wire diameter of 100 μ m was shorter than that with the wire diameter of 50 μ m. This is because the electric charge stored in the capacitance C_f at the rise/fall

time of the pulse voltage is the same at $q = C_f E_0$, where E_0 is the amplitude of the pulse voltage [15].

Figure 11 shows the machinable lengths of micro-rods with different diameters of wire tool electrode. When the feed speed of the workpiece in the axial direction was higher than 0.3 μ m/s, the machinable length was longer with the wire diameter of 50 μ m than 100 μ m. This is because the influence of stray current in the radial gap decreased with decreasing the wire diameter as shown in Fig. 10. Since the electric charge per pulse $q = C_f E_0$ is constant [15], more current flowed through the axial gap and used for the material removal with decreasing the wire diameter. Figure 12 shows the micro-rods machined with different wire diameters at the feed speed of 0.4 μ m/s. The machining process was completed with the preset feed distance of 300 μ m in the axial direction with the wire diameter of 50 μ m due to the less influence of stray current. However, the machining process was interrupted by collision between electrodes with the wire diameter of 100 μ m, resulting in a much shorter micro-rod length machined as shown in Fig. 12(b).

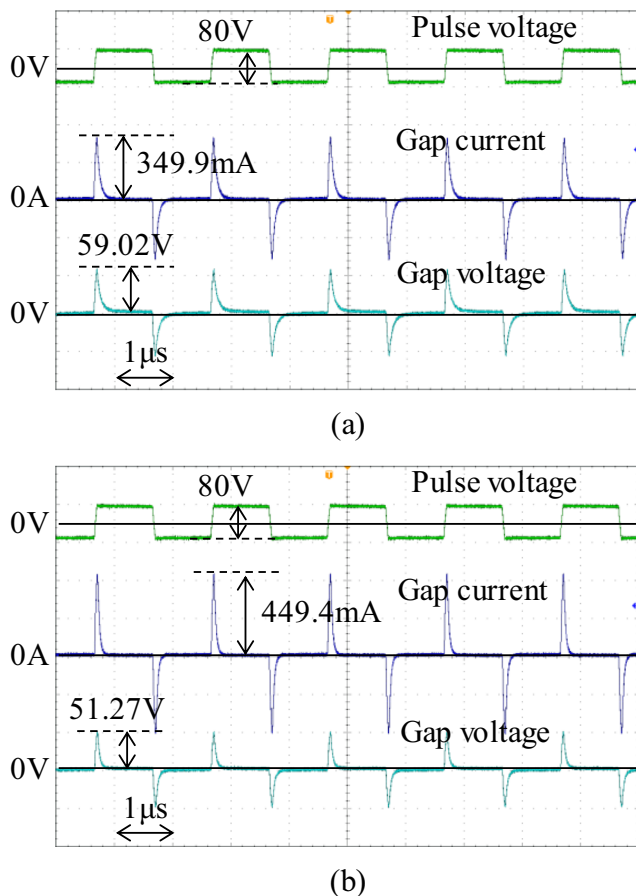


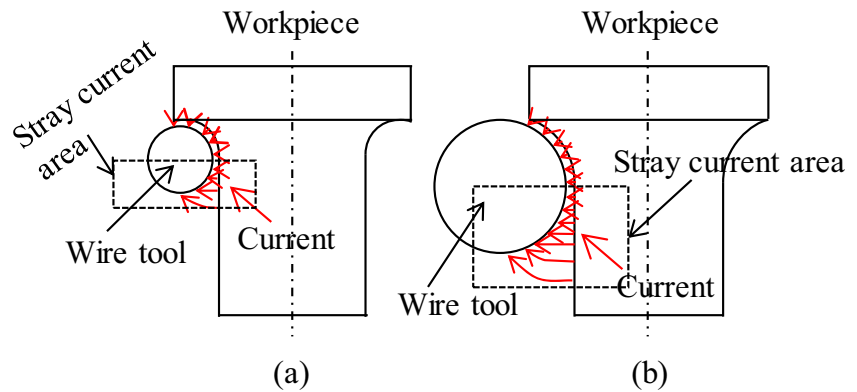
Fig. 9 Waveforms of gap current and voltage with different diameters of wire tool electrode. (a) Wire diameter of 50 μ m. (b) Wire diameter of 100 μ m

6 Influence of rotation speed of workpiece

6.1 Experimental method

Table 2 shows the experimental conditions to investigate the influence of the rotation speed of workpiece. Since many micro-rods were fabricated to complete this experiment and the reshaping process of tungsten rod workpiece from original diameter of 300 μ m to 200 μ m took a long time with the WEDG method, a pure tungsten rod in the original diameter of 125 μ m was purchased and used as the workpiece without the preprocess by WEDG. The amplitude of pulse voltage E_0 was reduced from the previous 80 V to 70 V corresponding to the decrease in the initial diameter of workpiece rod. This is because the electric charge q supplied to the gap is equal to $C_f E_0$. The rotation speed of workpiece rod was changed as 1915 rpm, 3000 rpm, and 3815 rpm. The NaNO₃ aqueous solution with concentration of 3 wt% was used as electrolyte and a SUS304 stainless steel wire of 50 μ m in diameter was used as tool electrode. The cut depth in the radial direction was 30 μ m to obtain nearly the same rod diameter of 50 μ m after machining as in Sections 3 and 4. The feed distance in the axial direction was 300 μ m. The rise/fall time of pulse voltage was 20 ns. The feed speed of workpiece was increased from 0.1 to 3.0 μ m/s with an interval of 0.5 μ m/s.

Fig. 10 Gap current distributions with different diameters of wire tool electrode. (a) Small wire diameter. (b) Large wire diameter



6.2 Experimental results

Figure 13 shows the waveforms of gap current and voltage with the workpiece rotation speeds of 1915 rpm and 3815 rpm. The gap current was increased slightly with increasing the rotation speed because the electrolyte refreshing in the narrow working gap was improved. The dissolved material and generated gas bubbles could be removed out of the working area sufficiently, hence, the gap resistance decreased, resulting in a higher current density.

The machinable lengths of micro-rods with different rotation speeds are shown in Fig. 14. There was an optimum feed speed for each rotation speed. This is because the micro-rod was totally shortened when the feed speed was too low due to the stray current flowing through the radial gap and the end of the micro-rod, while the machinable length was limited by collision between electrodes when the feed speed was excessively high. It is noted that the optimum feed speed increased with increasing the rotation speed of workpiece because the higher rotation speed improved the refreshing of electrolyte, resulting in increased current density due to smaller gap resistance. Figure 15 shows the micro-rods machined with different rotation speeds at the feed speed of 2 $\mu\text{m/s}$. The target feed distance of 300 μm was achieved with the rotation speed of

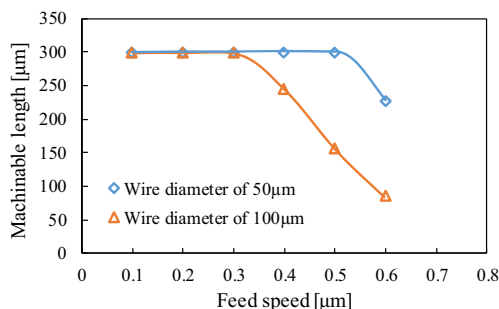


Fig. 11 Machinable lengths of micro-rod with different diameters of wire tool electrode

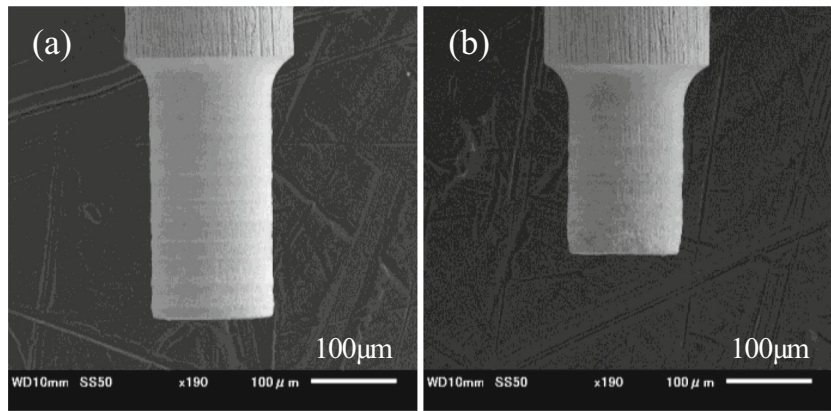
3815 rpm, but not with 1915 rpm. Figure 16 shows the wire tool electrodes before and after machining with different workpiece rotation speeds. The wear of the wire electrode was more significant with the higher rotation speed because of the higher current density. Considering the balance between the current density and the wear rate of the wire electrode, the workpiece rotation speed of 3000 rpm was used to investigate the influence of the frequency of pulse voltage on the machining characteristics in the next section.

7 Influence of pulse voltage frequency

The influence of the frequency of the pulse voltage was studied with different frequencies of 250 kHz, 400 kHz, 500 kHz, 600 kHz, and 1000 kHz. Figure 17 shows the waveforms of the gap current and voltage with the frequencies of 400 kHz and 1000 kHz at the feed speed of 1.5 $\mu\text{m/s}$. It is noted that when the frequency was 1000 kHz, the gap voltage failed to decrease to zero at the end of the positive pulse period, although the gap current can become zero as shown in Fig. 17(b). This is because oxide film was generated on the workpiece surface. Since the oxide film works as a capacitance, electric charge is stored in the capacitance. Hence, certain amount of electric charge is wasted to charge the capacitance, reducing the material removal amount per pulse.

Figure 18 shows the machinable lengths of micro-rods with different frequencies of pulse voltage. The machinable length of 0 μm means that the micro-rod could not be obtained because it was dissolved completely. It is found that there was an optimum feed speed for each frequency, with which the machinable length of micro-rod was longest. It is considered that the reason is the same as that caused the results shown in Fig. 14. Figure 19 shows the micro-rods machined with different frequencies at the feed speed of 1.5 $\mu\text{m/s}$. Figure 20 shows the corresponding machinable lengths. It shows that the maximum length

Fig. 12 Micro-rods machined with different wire diameters of (a) 50 μm and (b) 100 μm at the feed speed of 0.4 $\mu\text{m/s}$



of micro-rod was obtained at the optimum frequency of 500 to 600 kHz. It is also found in Fig. 18 that the optimum feed speed increased with increasing the frequency. The electric charge per pulse is constant at $q = C_p E_0$. Hence, if the material removal per pulse can be kept constant, the material removal rate should be in proportion to the frequency. However, the optimum feed speed was not doubled when the frequency was increased from 500 to

1000 kHz. Furthermore, the machinable length was less than the preset feed distance of 300 μm even at the optimum feed speed because of the collision between electrodes with the highest frequency of 1000 kHz. Figure 21 shows the longest micro-rod of 250 μm obtained with the frequency of 1000 kHz at the optimum feed speed of 2 $\mu\text{m/s}$. The machining accuracy was also low. This is probably because the removal per pulse was decreased at 1000 kHz because some amount of charge was wasted to charge the oxide film as described above.

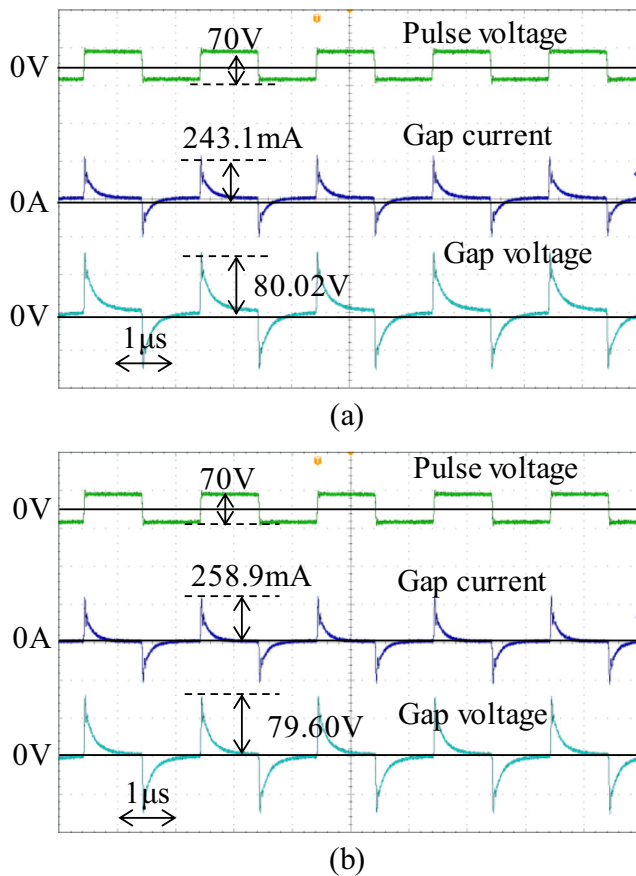


Fig. 13 Waveforms of gap current and voltage with different rotation speeds of workpiece rod. (a) Rotation speed of 1915 rpm. (b) Rotation speed of 3815 rpm

8 Machinable minimum diameter using WECT method

8.1 Experimental method

The experimental conditions in Table 2 were used in this section. The rotation speed of workpiece rod was 3000 rpm, and the feed speed of workpiece was 0.1 $\mu\text{m/s}$. The target diameters of the machined micro-rods were 10 μm , 20 μm , 30 μm , 40 μm , and 50 μm , which were changed by the cut depth in the radial direction shown in Fig. 2.

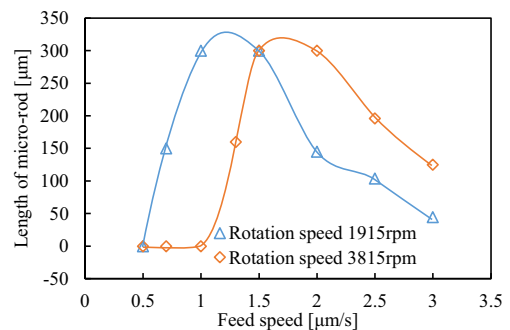


Fig. 14 Machinable lengths of micro-rods with different rotation speeds of workpiece rod

Fig. 15 Micro-rods machined with rotation speeds of (a) 1915 rpm and (b) 3815 rpm at the feed speed of 2 $\mu\text{m/s}$

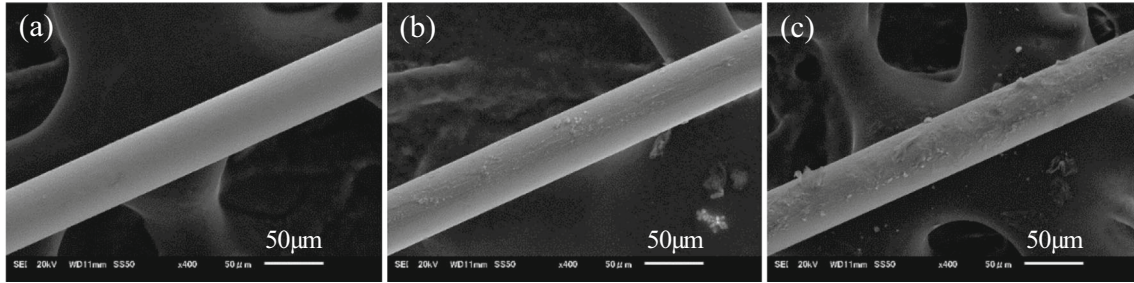
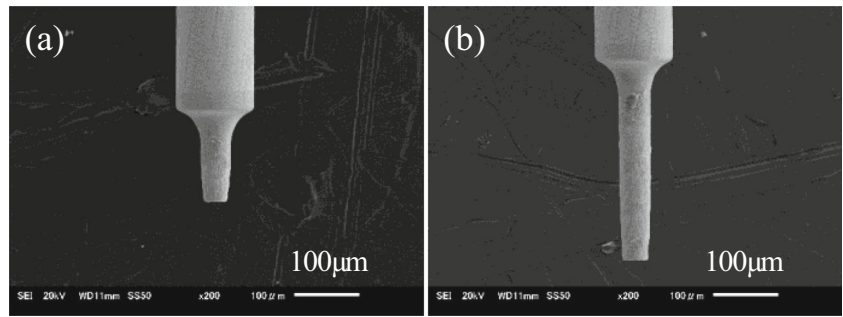


Fig. 16 Wire tool electrodes (a) before machining and after machining with workpiece rotation speeds of (b) 1915 rpm and (c) 3815 rpm

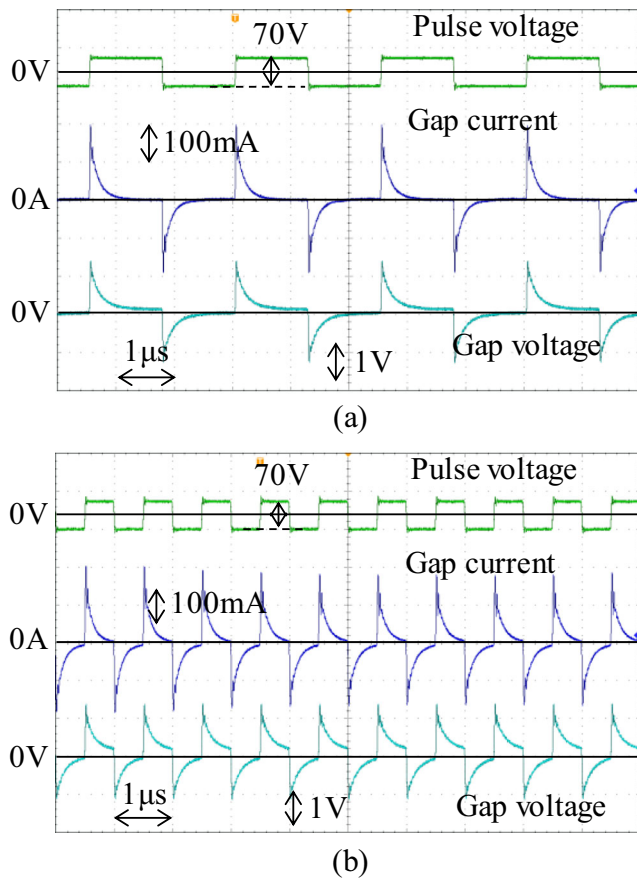


Fig. 17 Waveforms of gap current and voltage with frequencies of 400 kHz and 1000 kHz. (a) Frequency of 400 kHz. (b) Frequency of 1000 kHz

8.2 Experimental results

Figure 22 shows the relationship between target rod diameter and machined rod diameter. The deviation of rod diameter was caused by the positioning error of the equipment and the inconsistency of the working gap width between the workpiece and wire tool electrodes. When the target diameter was smaller than 30 μm , the machining process never succeeded to obtain a micro-rod. Thus, the minimum diameter of machined micro-rod was 11 μm . Figure 23 shows the machined micro-rod with the minimum diameter. A high aspect ratio of 36 was obtained with the proposed WECT method. The diameter and length of the micro-rod were 11 μm and 400 μm , respectively. It is noted that the machined micro-rod is slightly

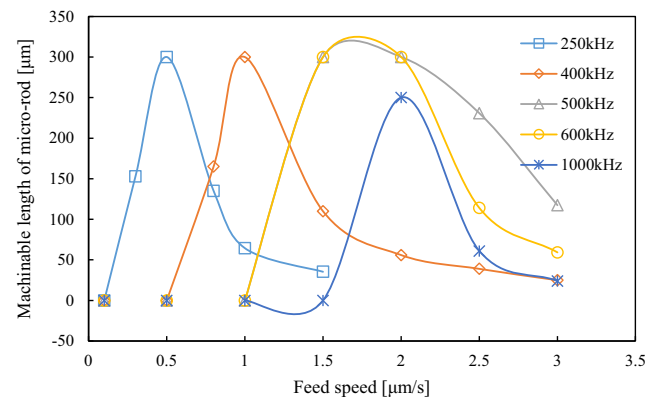
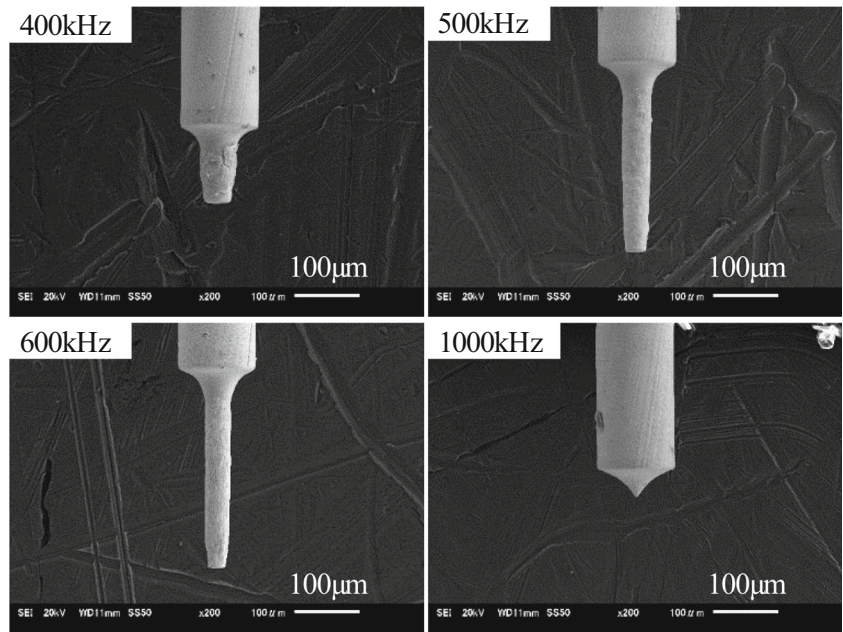


Fig. 18 Machinable lengths of micro-rod with different frequencies

Fig. 19 Micro-rods machined with different frequencies at feed speed of 1.5 μm/s



bent. It is considered this was caused by the residual stress which existed in the rod workpiece prior to machining due to the wire drawing process to produce the tungsten rod purchased.

In the authors’ previous research, a platinum film of 20 μm in thickness was used as the tool electrode to fabricate tungsten micro-rods with a neutral electrolyte and bipolar pulse current [21], in which two steps were used to obtain the minimum diameter. Figure 24 shows the machined minimum diameter of 5.6 μm with the length of 100 μm. Compared with the WECT method, a less diameter was obtained because the film tool thickness of 20 μm was less than the wire diameter of 50 μm, resulting in less influence of stray current during machining process. However, since the platinum

tool electrode was worn with the bipolar current, the maximum aspect ratio was 18, much lower than 36 with the WECT method.

9 Conclusions

The wire electrochemical turning (WECT) method was used to machine tungsten micro-rods using a neutral electrolyte and bipolar current in this research. Since the wire tool electrode was kept being wound during the machining process, the influence of tool wear due to the bipolar pulse current was

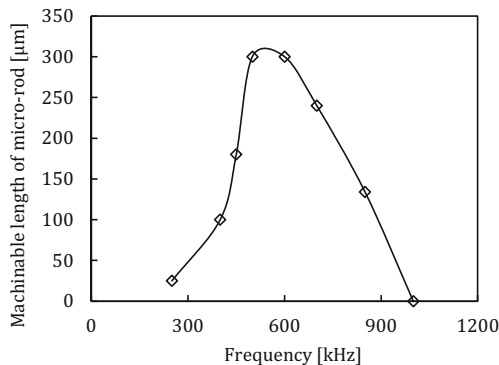


Fig. 20 Machinable lengths of micro-rods with different frequencies at feed speed of 1.5 μm/s

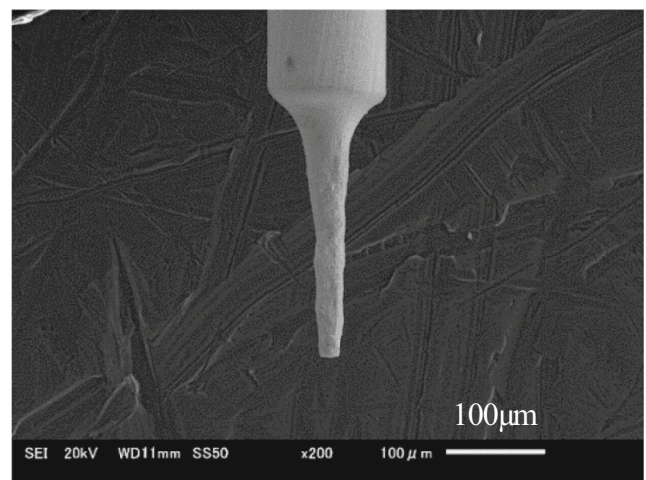


Fig. 21 Micro-rods machined with frequency of 1000 kHz at optimum feed speed of 2 μm/s

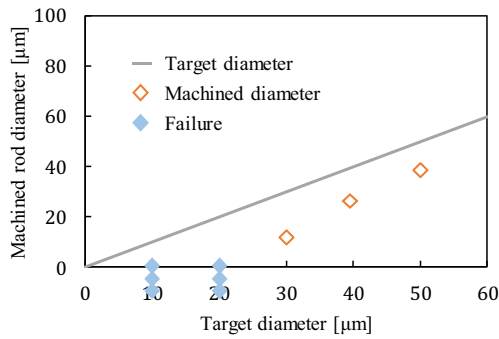


Fig. 22 Relationship between target rod diameter and machined rod diameter

eliminated. According to the experimental results, the following conclusions were obtained.

- (1) The machining efficiency of tungsten micro-rods was higher with the NaCl electrolyte than with the NaNO₃ electrolyte due to the high current efficiency of NaCl aqueous solution. However, the machining accuracy of NaNO₃ was better due to the narrower working gap width.
- (2) The machining accuracy was higher with the SUS304 stainless steel wire electrode than the brass wire electrode due to the less tool wear caused by the bipolar pulse current.
- (3) The current efficiency and machining accuracy were improved with decreasing the diameter of the wire tool electrode because the influence of the stray current flowing through the radial gap and the end of micro-rod was decreased.
- (4) The machining efficiency was increased with increasing the rotation speed of the workpiece rod because the refreshing of electrolyte in the narrow working gap was improved. However, more tool

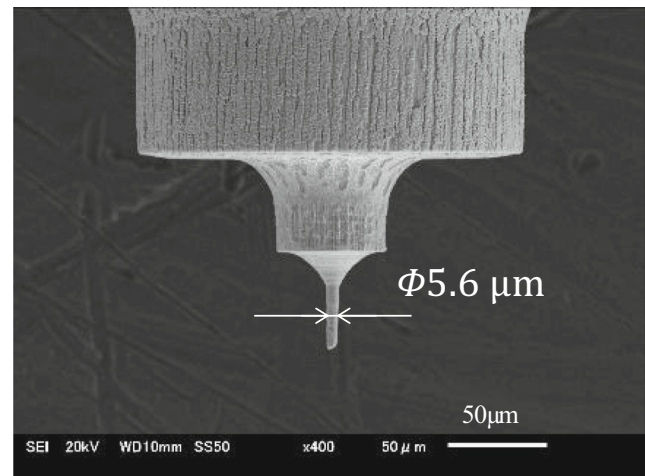


Fig. 24 Micro-rods machined with platinum film tool electrode [21]

- material was dissolved, when the polarity of the wire tool electrode was positive, due to the higher current density.
- (5) There was an optimum feed speed of workpiece rod in the axial direction with which the longest rod was obtained, and this optimum feed speed increased with increasing the frequency of pulse voltage.
 - (6) The material removal rate increased in proportion to the pulse frequency until 500 kHz. However, further increase in the frequency resulted in decrease of material removal per pulse because of the charge stored in the capacitance due to the oxide film.
 - (7) With the WECT method, the minimum rod diameter of 11 μm was obtained with a high aspect ratio of 36 because the influence of tool wear caused by the bipolar pulse current was eliminated with the winding wire tool electrode. Compared with the previous platinum film tool electrode method, the aspect ratio was increased by twice.

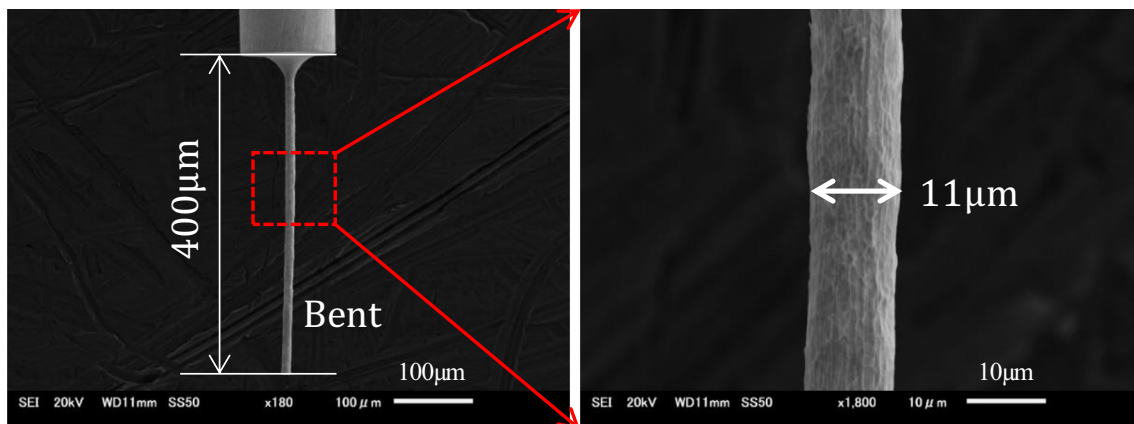


Fig. 23 Machined micro-rod with minimum diameter of 11 μm

Acknowledgments The authors would like to thank Dr. Takeshi Masaki for his kind help in installing the wire winding system for this research.

Funding This work was supported by the Cross-Ministerial Strategic Innovation Promotion Program (SIP): Innovative Design/Manufacturing Technologies, funded by NEDO.

References

- Ren C, Fang ZZ, Koopman M, Butler B, Paramore J, Middlemas S (2018) Methods for improving ductility of tungsten - a review. *Int J Refract Met Hard Mater* 75:170–183. <https://doi.org/10.1016/j.ijrmhm.2018.04.012>
- Cardarelli F (2008) *Materials handbook: a concise desktop reference*. Springer Science & Business Media
- Federici G, Zhitlukhin A, Arkhipov N, Giniyatulin R, Klimov N, Landman I, Podkovyrov V, Safronov V, Loarte A, Merola M (2005) Effects of ELMs and disruptions on ITER divertor armour materials. *J Nucl Mater* 337–339:684–690. <https://doi.org/10.1016/j.jnucmat.2004.10.149>
- Zhong L, Li L, Wu X, He N (2017) Micro cutting of pure tungsten using self-developed polycrystalline diamond slotting tools. *Int J Adv Manuf Technol* 89:2435–2445. <https://doi.org/10.1007/s00170-016-9292-y>
- Yang RT, Tzeng CJ, Yang YK, Hsieh MH (2012) Optimization of wire electrical discharge machining process parameters for cutting tungsten. *Int J Adv Manuf Technol* 60:135–147. <https://doi.org/10.1007/s00170-011-3576-z>
- Garg RK, Singh KK, Sachdeva A, Sharma VS, Ojha K, Singh S (2010) Review of research work in sinking EDM and WEDM on metal matrix composite materials. *Int J Adv Manuf Technol* 50:611–624. <https://doi.org/10.1007/s00170-010-2534-5>
- Kunieda M, Lauwers B, Rajurkar KP, Schumacher BM (2005) Advancing EDM through fundamental insight into the process. *CIRP Ann* 54:64–87. [https://doi.org/10.1016/S0007-8506\(07\)60020-1](https://doi.org/10.1016/S0007-8506(07)60020-1)
- Rajurkar KP, Zhu D, McGeough JA et al (1999) New developments in electro-chemical machining. *CIRP Ann - Manuf Technol* 48:567–579. [https://doi.org/10.1016/S0007-8506\(07\)63235-1](https://doi.org/10.1016/S0007-8506(07)63235-1)
- Lim YM, Kim SH (2001) An electrochemical fabrication method for extremely thin cylindrical micropin. *Int J Mach Tools Manuf* 41:2287–2296. [https://doi.org/10.1016/S0890-6955\(00\)00129-2](https://doi.org/10.1016/S0890-6955(00)00129-2)
- Fan ZW, Hourng LW, Wang CY (2010) Fabrication of tungsten microelectrodes using pulsed electrochemical machining. *Precis Eng* 34:489–496. <https://doi.org/10.1016/j.precisioneng.2010.01.001>
- Maeda S, Saito N, Haishi Y (1967) Principle and characteristics of electro-chemical machining. *Tech Rep Mitsubishi Electr* 41:1267–1279
- Han W, Kunieda M (2017) Fabrication of tungsten micro-rods by ECM using ultra-short-pulse bipolar current. *CIRP Ann - Manuf Technol* 66:193–196. <https://doi.org/10.1016/j.cirp.2017.04.131>
- Kunieda M, Hayasaka A, Yang XD, Sano S, Araie I (2007) Study on nano EDM using capacity coupled pulse generator. *CIRP Ann - Manuf Technol* 56:213–216. <https://doi.org/10.1016/j.cirp.2007.05.051>
- Schuster R, Kirchner V, Allongue P, Ertl G (2000) Electrochemical micromachining. *Science* (80-) 289:98–101. <https://doi.org/10.1126/science.289.5476.98>
- Koyano T, Kunieda M (2013) Micro electrochemical machining using electrostatic induction feeding method. *CIRP Ann - Manuf Technol* 62:175–178. <https://doi.org/10.1016/j.cirp.2013.03.107>
- Han W, Kunieda M (2018) Wire electrochemical grinding of tungsten micro-rods using neutral electrolyte. *Precis Eng* 52:458–468. <https://doi.org/10.1016/j.precisioneng.2018.02.006>
- Masuzawa T, Fujino M, Kobayashi K, Suzuki T, Kinoshita N (1985) Wire electro-discharge grinding for micro-machining. *CIRP Ann - Manuf Technol* 34:431–434. [https://doi.org/10.1016/S0007-8506\(07\)61805-8](https://doi.org/10.1016/S0007-8506(07)61805-8)
- Mayank G, Fuchen C, Masanori K (2018) Analysis of reactions determining current efficiency in electrochemical machining. *Procedia CIRP*, In, pp 511–516
- Sato T (1970) *Electrochemical machining and chemical machining*. Asakura Publishing
- Han W, Kunieda M (2017) Research on improvement of machining accuracy of micro-rods with electrostatic induction feeding ECM. *Precis Eng* 50:494–505. <https://doi.org/10.1016/j.precisioneng.2017.07.005>
- Han W, Kunieda M (2017) Tungsten machining with electrostatic induction feeding ECM. In: 7th International Conference of Asian Society for Precision Engineering and Nanotechnology. pp 14–17

Publisher's note Springer Nature remains neutral with regard to jurisdictional claims in published maps and institutional affiliations.